International Journal of Microwave and Wireless Technologies

cambridge.org/mrf

Compact circularly polarized antenna with wide axial ratio bandwidth using modified quasi-self-complementary structure

Gunjan Srivastava

Department of Electronics and Electrical Communication Engineering, Indian Institute of Technology Kharagpur, West Bengal-721302, India

Research Paper

Cite this article: Srivastava G (2019). Compact circularly polarized antenna with wide axial ratio bandwidth using modified quasi-self-complementary structure. *International Journal of Microwave and Wireless Technologies* **11**, 35–40. https://doi.org/10.1017/S175907871800106X

Received: 13 September 2017
Revised: 22 June 2018
Accepted: 22 June 2018
First published online: 26 July 2018

Key words:
Circular polarization; wide axial ratio bandwidth; QSC antenna

Author for correspondence:
Gunjan Srivastava, E-mail: gunjansri21@gmail.com

A compact circularly polarized antenna with wide axial ratio bandwidth (ARBW) using quasi-self-complementary (QSC) structure is presented. A 3-dB ARBW is achieved by shortening the ground plane of the QSC structure. Furthermore, the wide ARBW is obtained by the introduction of a stepped stub in the extended ground plane of the QSC structure. The antenna is fabricated on a FR4 substrate with the overall dimensions of 25 mm × 22 mm × 0.8 mm. The proposed antenna has an impedance bandwidth of 5.9 GHz (2.4–8.3 GHz, 110%) and 3 dB ARBW of 1.6 GHz (2.4–4 GHz, 50%). A peak gain of 1–3 dBi is observed within the 3 dB ARBW.

Introduction

Modern communication systems such as GPS, RFID, WLAN, WiMAX, etc. require circularly polarized (CP) antennas. CP antennas have better immunity toward multipath fading and polarization mismatch as compared with linearly polarized (LP) antennas [1]. In CP radiations, two orthogonal modes with equal amplitude which are 90° out of phase are excited. CP antennas can be broadly classified into two types: single fed or dual fed antennas. For the dual fed CP antennas, a 90° hybrid is required to have the essential phase shift of 90°. Dual fed antennas have complex designs, larger size, and higher losses [2]. Thus, single fed CP antennas are more preferred over the dual fed antennas. Several single fed CP antennas have been reported in the literature. The two orthogonal modes with equal amplitude with 90° phase difference can be achieved by introducing an asymmetry and/or perturbations in different monopoles [3–8] and slot antennas [9–11] in single fed antennas. A single microstrip fed CP square patch antenna with a pair of truncated corners analyzed and designed using a multiport network model is presented in [3]. In [4], CP radiations are obtained by cutting slits of a square patch. A microstrip fed CP antenna with a cross-shaped slot is presented in [5]. All the above reported works have mostly narrow 3 dB-axial ratio bandwidths (ARBW).

With the advancement of communication technology, CP antennas with a wide impedance bandwidth and wide ARBW are in great demand [6–11]. In [6], a trapezoidal structure is presented which possess both the CP (ARBW = 8%) and LP radiations. In [9], a broadband coplanar waveguide fed CP slot antenna with an open slot having an ARBW of 27% is presented. However, their larger size and complex design restrict its application in portable wireless devices. Two orthogonal degenerate modes in [10] are generated by protruding the square shaped slot with a metallic stub and the asymmetric microstrip feed line with 40% ARBW. An ARBW of 44.9% is achieved in coplanar waveguide (CPW) fed planar monopole antenna by adding a vertical stub and cutting a horizontal slit on the ground plane [7]. However, designing a compact CP monopole antenna with the wide impedance bandwidth as well as wide ARBW is a true challenge for antenna designers.

A self-complementary antenna was initially reported in [12] along with its frequency-independent broadband characteristics. Self-complementary concepts were applied over a monopole or a slot for size miniaturization in [13]. Later, the quasi-self-complementary (QSC) structures are employed to obtain wide or multi-band impedance characteristics [14–16] in compact dimensions. Here, the QSC structure is employed to obtain a wide impedance bandwidth along with wide 3 dB ARBW characteristics.

In this paper, a compact CP modified QSC antenna with a wide 3 dB ARBW is presented. The wideband circular polarization of the proposed antenna is achieved by asymmetrical QSC structure and the stepped stub attached to its extended ground plane. In the present design, a 3 dB ARBW of 1.6 GHz is obtained which is nearly 50% (relative to the center frequency of 3.2 GHz). The proposed antenna is suitable for several wireless communication systems such as 2.4 GHz WLAN (2400–2484 MHz), WiMAX (2500–2690 MHz, 3200–3800 MHz) bands, etc.

© Cambridge University Press and the European Microwave Association 2018

CAMBRIDGE UNIVERSITY PRESS

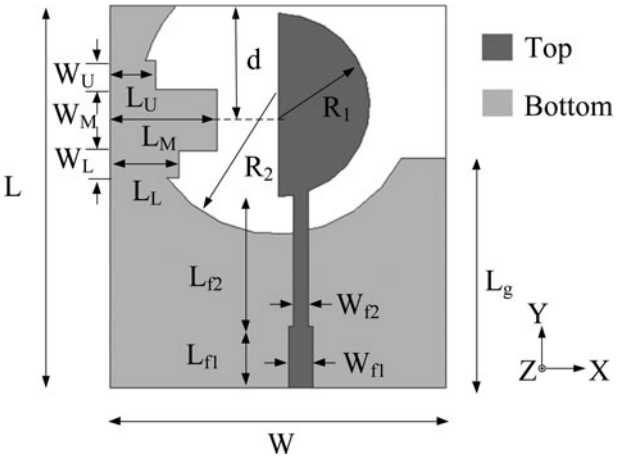


Fig. 1. Geometry of the proposed CP antenna.

Antenna configuration

The geometry of the proposed CP antenna is shown in Fig. 1. It is fed by a 50 Ω microstrip feed line printed on the top of the substrate. A low cost FR4 substrate having a dielectric constant of 4.4, loss tangent of 0.02, and thickness of 0.8 mm is used in the present design. The overall size of the proposed antenna is 25 mm × 22 mm. The proposed antenna is the modified QSC structure, which consists of a semi-circular patch of radius R_1 and a modified complementary etched ground plane of radius R_2 with a stepped stub attached to its extended ground plane as shown in Fig. 1. Figure 2 shows the evolution of the proposed structure from the basic QSC structure to the final wideband CP antenna. The S_{11} parameters and the axial ratio of the different antennas shown in Fig. 2 are plotted in Fig. 3.

It is well-known that a QSC structure based antenna exhibits the wide impedance bandwidth. The basic QSC structure (Ant-I) resonates at two frequencies: 3.5 and 7.2 GHz. Ant-I

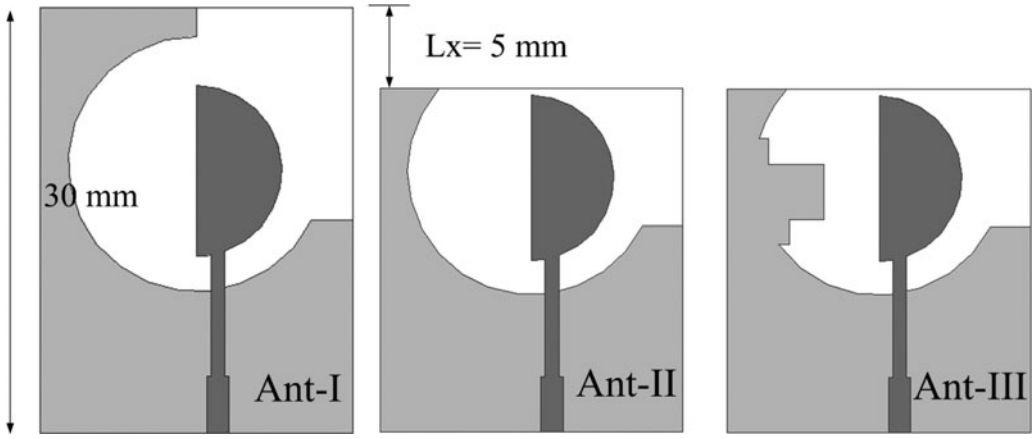


Fig. 2. Evolution of the proposed antenna: (a) Ant-I, (b) Ant-II, and (c) Ant-III.

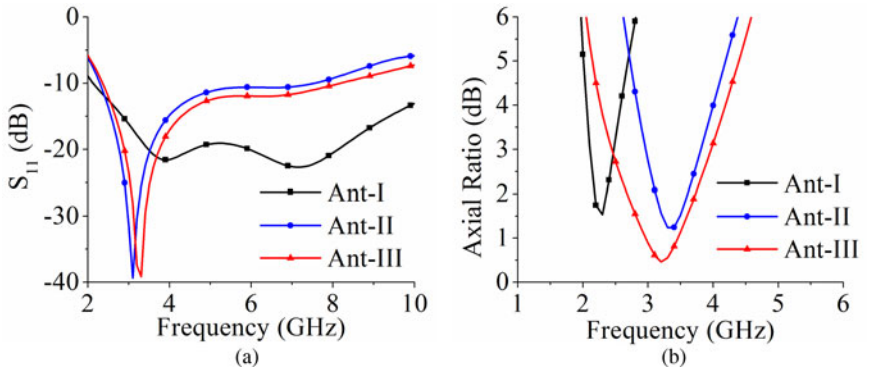


Fig. 3. Simulated (a) S_{11} parameters and (b) axial ratio for Ant-I, Ant-II, and Ant-III.

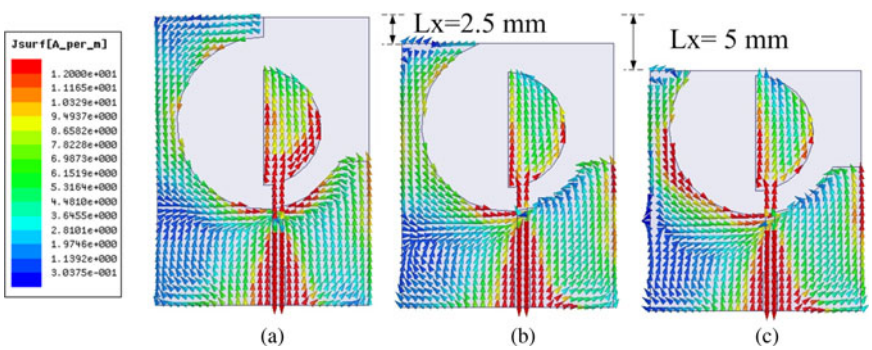


Fig. 4. Surface current distribution for different values of L_x at 3.5 GHz: (a) L_x = 0 mm, (b) L_x = 2.5 mm, and (c) L_x = 5 mm.

https://doi.org/10.1017/S175907871800106X Published online by Cambridge University Press

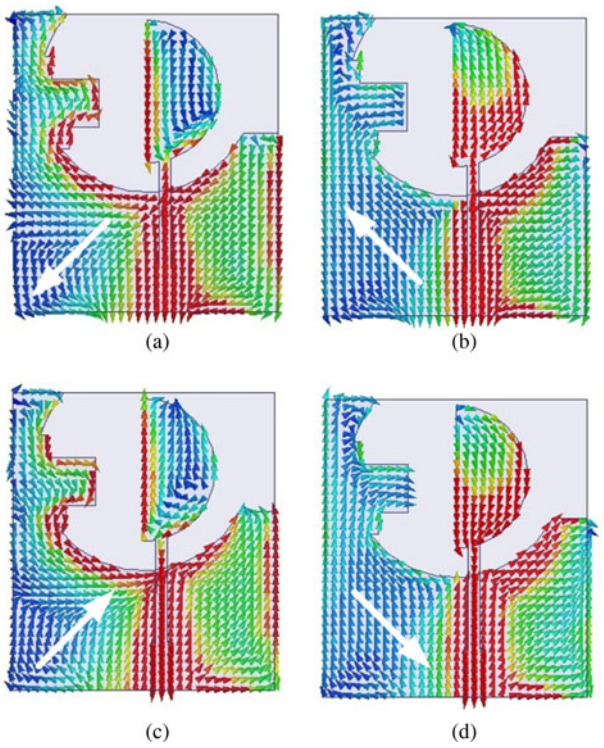


Fig. 5. Simulated surface current distribution of the proposed antenna at 3.5 GHz for (a) $\omega t = 0°$, (b) $\omega t = 90°$, (c) $\omega t = 180°$, and (d) $\omega t = 270°$.

has an asymmetrical ground plane that results in narrow band CP radiations (3-dB ARBW = 2.1–2.5 GHz, 17.4%) [9]. At the first resonant frequency, 3.5 GHz, Ant-I mainly have vertically polarized radiations. It is due to the presence of oppositely oriented horizontal currents in the ground plane which cancels each other and results in vertically polarized radiations [Fig. 4(a)].

In order to obtain CP radiations, the extended ground plane along with the substrate of the basic QSC structure is shortened by L_x [Fig. 2(b)]. The surface current distributions at 3.5 GHz for $L_x = 2.5$ mm and $L_x = 5$ mm are plotted in Fig. 4(b) and (c), respectively. As the value of L_x increases, the resultant horizontal currents are generated in the ground plane. For $L_x = 5$ mm (Ant-II), a significant amount of horizontal currents is produced which along with vertical currents results in CP radiations. Thus, the shortening of the ground plane not only reduces the size of the antenna, but also results in CP radiations.

The impedance bandwidth of Ant-II is from 2.3–7.6 GHz, while the 3-dB ARBW is 2.9–3.8 GHz, which is nearly 26.9%. Furthermore, to enhance ARBW, a stepped stub is introduced in the extended ground plane (Ant-III). This stepped stub creates an equal horizontal current in-phase quadrature with the vertical currents, that results in a wideband 3-dB ARBW (2.4–4.0 GHz, 50%).

Circular polarization mechanism

In order to understand the operating principle of the proposed antenna, the time varying surface currents of the proposed antenna at 3.5 GHz are plotted in Fig. 5. As reported in literature

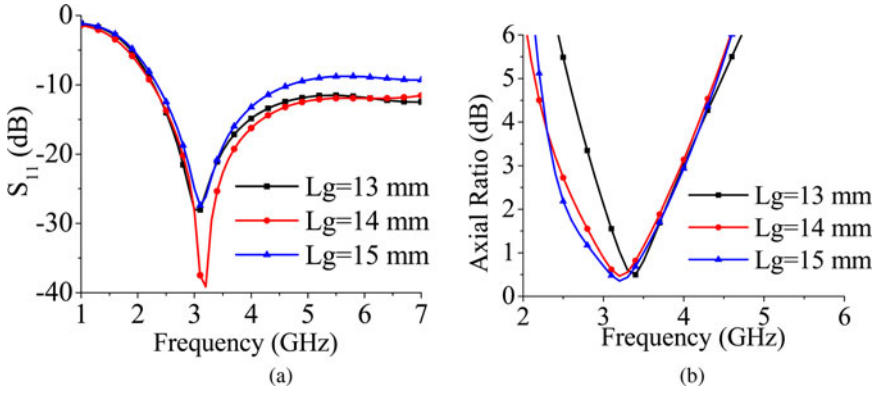


Fig. 6. Simulated (a) S_{11} parameters and (b) axial ratio for different values of L_g.

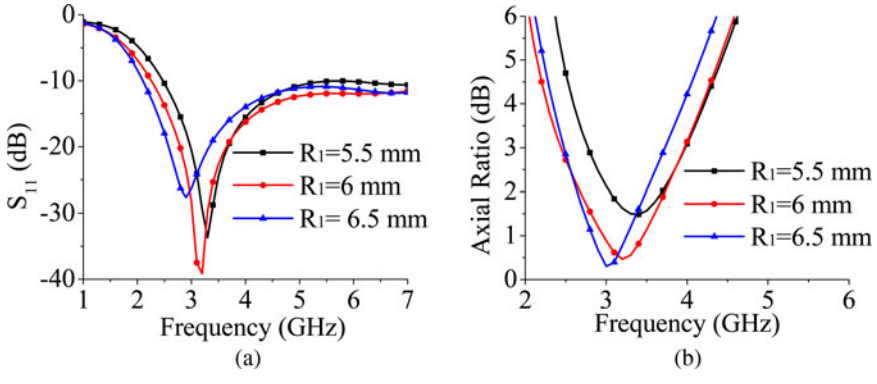


Fig. 7. Simulated (a) S_{11} parameters and (b) axial ratio for different values of R_1.

https://doi.org/10.1017/S175907871800106X Published online by Cambridge University Press

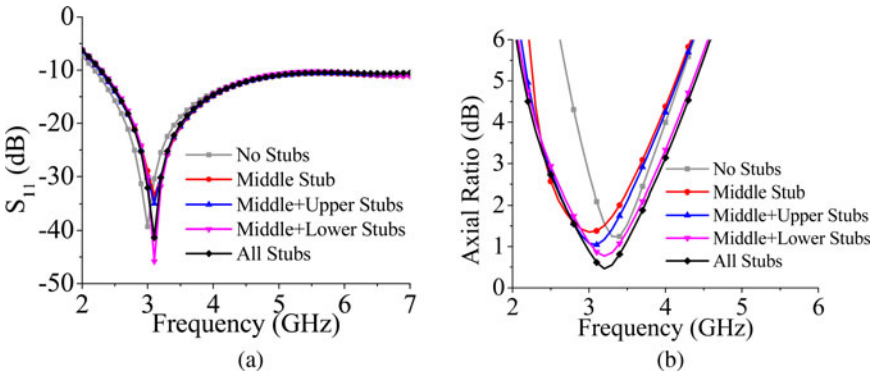


Fig. 8. Simulated (a) S_{11} parameters and (b) axial ratio for combination of different stubs.

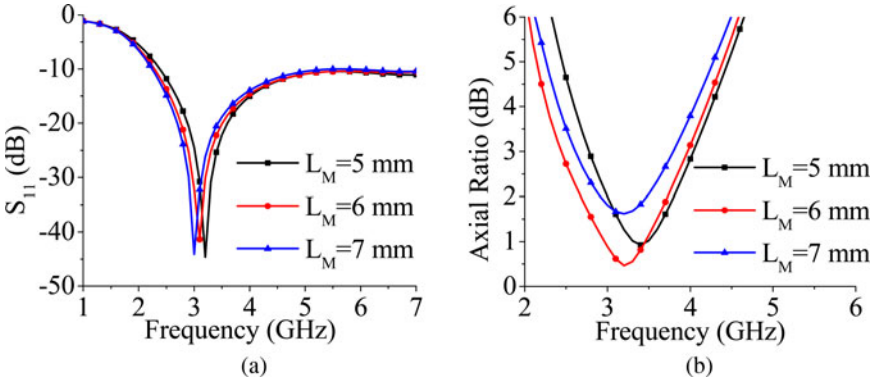


Fig. 9. Simulated (a) S_{11} parameters and (b) axial ratio for different values of L_M.

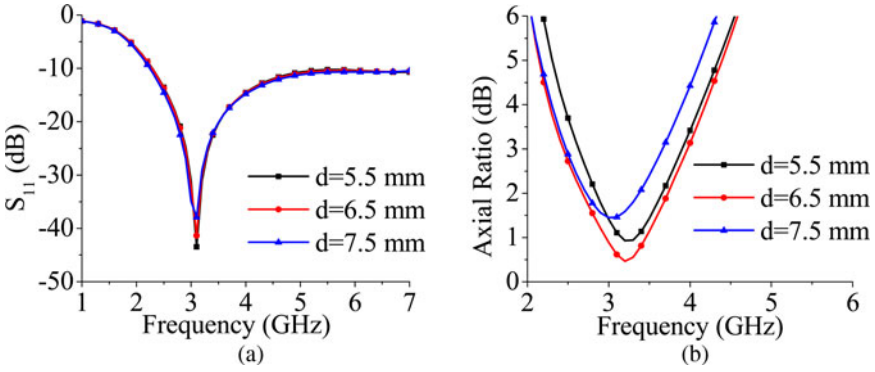


Fig. 10. Simulated (a) S_{11} parameters and (b) axial ratio for different values of d.

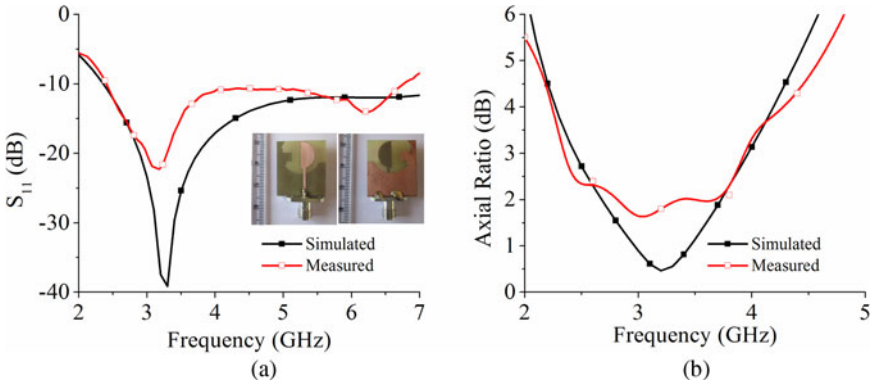


Fig. 11. Simulated and measured (a) S_{11} parameter and (b) axial ratio.

https://doi.org/10.1017/S175907871800106X Published online by Cambridge University Press

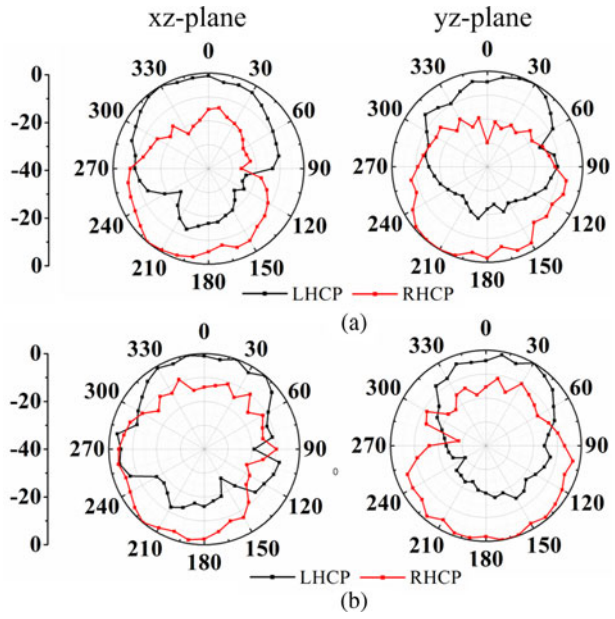


Fig. 12. Measured radiation patterns of the proposed antenna at (a) 2.8 GHz and (b) 3.5 GHz.

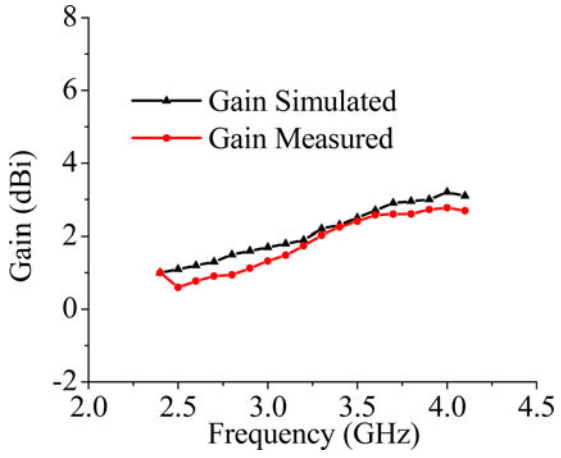


Fig. 13. Simulated and measured gain of the proposed antenna.

[9], the asymmetry in the ground plane as well as asymmetry in the feed line will result in wideband CP operation. It can be observed that the surface currents rotating in the clockwise direction results left-hand CP (LHCP) radiation in the $+z$-direction and right-hand CP (RHCP) radiation in the $-z$-direction.

Parametric analysis

In order to understand the basic underlying principle of the proposed CP antenna, the parametric study of different geometrical parameters is conducted for a wide impedance bandwidth and wide 3 dB ARBW. The effects of different geometrical parameters are discussed as follows to obtain the final dimensions of the proposed antenna.

Effect of ground plane parameter, L_g

The variations in parameter L_g of the ground plane greatly influence antenna's $|S_{11}|$ characteristics and AR as shown in Fig. 6. The increase in the value of L_g affects the impedance matching at the upper frequency edge, while the resonant frequency at the lower frequency remains almost unaltered. Whereas, the ARBW improves at the lower frequency edge as L_g increases. Hence, by considering the trade-off between the impedance bandwidth and ARBW, $L_g = 14$ mm is chosen as an optimal design parameter.

Effect of radius of semi-circular feed structure, R_1

The radius R_1 of the semi-circular feed structure also affects the antenna's $|S_{11}|$ and AR as shown in Fig. 7. It can be observed that an increase in the value of R_1, shifts the lower frequency edge of S_{11} curve toward the lower value. The value of $R_1 =$ 6 mm provides the wide ARBW, hence it is chosen as an optimal design parameter.

Effect of introduction of a stepped stub

The effects of the stepped stub on the S_{11} parameter and axial ratio performance are presented in Fig. 8. The stepped stub can be divided into three smaller stubs: upper stub, middle stub, and lower stub. First, the middle stub is introduced at the central position of the extended ground plane. Subsequently, the upper and lower stubs are added separately to evaluate their effects on antenna's performance. Finally, all the three stubs are applied together to obtain our designed antenna. It can be observed from Fig. 8(a) that with the introduction of stubs S_{11} curve shifts toward the right with a slight change in the impedance bandwidth. While the introduction of stubs has a significant effect on the axial ratio performance of the antenna. The 3 dB ARBW is maximum (1.6 GHz) for the combination of all the three stubs, i.e. stepped stub.

Effect of length of middle stub, L_M

The variation of the length L_M of middle stub on the S-parameters and axial ratio performance is plotted in Fig. 9. It can be observed that as the value of L_M increases, S_{11} curve shifts toward the left. The ARBW is maximum when the value of L_M equals 6 mm. Hence, $L_M = 6$ mm is an optimum choice for the proposed design.

Effect on the position of stepped stub, d

The position of the stepped stub 'd' is optimized in this section. As can be seen from Fig. 10(a), there is insignificant effect on S_{11} characteristics of the proposed antenna. It can be observed from Fig. 10(b) that the ARBW is maximum for the value of d = 6.5 mm. Thus, $d = 6.5$ mm is chosen as an optimal design parameter for the position of the stepped stub.

The optimized parameters of the proposed antenna are: $L =$ 25 mm, $W = 22$ mm, $L_{f1} = 4$ mm, $L_{f2} = 8.6$ mm, $W_{f1} = 1.6$ mm, $W_{f2} = 1$ mm, $L_g = 14$ mm, $R_1 = 6$ mm, $R_2 = 9$ mm, $W_U = 1.9$ mm, $L_U = 3$ mm, $W_M = 4$ mm, $L_M = 7$ mm, $W_L = 1.8$ mm, $L_L =$ 4.5 mm, and $d = 6.5$ mm.

Results and discussions

In order to verify the present design approach, the proposed antenna with the optimized design parameters is fabricated and its radiation characteristics are measured. The simulated and

https://doi.org/10.1017/S175907871800106X Published online by Cambridge University Press

Table 1. A comparison of the proposed CP antenna with other CP antennas

Ref.	Substrate ε_r, thickness (mm)	Impedance BW (GHz) (%)	3 dB ARBW (GHz) (%)	Antenna area (mm × mm), λ_0^2	Peak gain (dBi)
[8]	FR4 4.4, 1.0	1.48–4.24, 96.5	2.05–3.95, 63.3	55 × 50, 0.27 × 0.24	0.5–3.5
[9]	FR4 4.4, 0.8	2.13–7.46, 92	3.2–4.2, 27	50 × 50, 0.35 × 0.35	4.75–5.60
[10]	FR4 4.4, 1.6	3.5–9.25, 90.2	4.6–6.9, 40	25 × 25, 0.23 × 0.23	0.8–4.5
[11]	RT/Duroid 4.4, 1.6	3.25–8, 84	4.4–6.67, 41.3	28 × 28, 0.30 × 0.30	3.0–3.75
This work	FR4 4.4, 0.8	2.4–8.3, 110	2.4–4.0, 50	25 × 22, 0.20 × 0.18	0.5–3.2

measured results are shown in Fig. 11 and there is a good agreement between them. The measured impedance bandwidth is 4.36 GHz (2.43–6.79 GHz, 95%). The standard laboratory procedure described in [17] has been adapted for axial ratio measurements. The simulated and measured axial ratio performances in the broadside direction are shown in Fig. 11(b). The measured ARBW is 1.5 GHz (2.4–3.9 GHz, 48%).

The measured far field radiation patterns of the proposed antenna in the *xz*- and *yz*-planes at 2.8 and 3.5 GHz are shown in Fig. 12. It is clear from the figure that the antenna exhibits a bidirectional radiation with opposite circular polarizations. The antenna has LHCP radiations for $z > 0$, which provides maximum radiations nearly in the broadside direction. While it has RHCP radiations for $z < 0$, which provides the maximum radiations approximately at $\phi = 0°$ and $\theta = 180°$. The peak gain of the proposed antenna is plotted in Fig. 13. The antenna has the peak gain of 3 dBi with a variation of 1–2 dB within the 3 dB ARBW. The antenna gain is low at the lower frequencies, due to its smaller dimensions, which indicates the tradeoff between the gain bandwidth and its dimensions. In the middle and higher frequencies, the gain varies between 2 and 3 dBi.

Table 1 lists a comparison of the proposed antenna with the other similar antennas reported in the literature. It can be observed from the table that the proposed antenna has comparable or better performance over the other antennas in terms of either size or ARBW.

Conclusion

A compact wideband CP antenna using a modified QSC structure is designed, fabricated, and its characteristics are measured. The proposed antenna has a wide impedance bandwidth (110%) and wide ARBW (50%). The asymmetrical modified QSC structure and the stepped stub attached in its extended ground plane result in wideband CP radiations. The measured results show that the presented CP antenna will be a potential candidate for WLAN bands (2400–2484 MHz) and WiMAX bands (2500 MHz–2690 MHz, 3200–3800 MHz).

References

1. **Chang F-S, Wong K-L and Chiou T-W** (2003) Low-cost broadband circularly polarized patch antenna. *IEEE Transactions on Antennas and Propagation* **51**, 3006–3009.
2. **Garg R, Bhartia P, Bahl I and Ittipiboon A** (2001) *Microstrip Antenna Design Handbook*. Norwood, MA: Artech House.
3. **Sharma PC and Gupta KC** (1983) Analysis and optimized design of single feed circularly polarized microstrip antenna. *IEEE Transactions on Antennas and Propagation* **29**, 949–955.
4. **Wong K-L and Wu J-Y** (1997) Single feed Small circularly polarised square microstrip antenna. *Electronics Letters* **33**, 1833–1834.
5. **Iwasaki H** (1996) A circularly polarized small-sized microstrip antenna with a cross-slot. *IEEE Transactions on Antennas and Propagation* **44**, 1399–1401.
6. **Augustin G and Denidni TA** (2012) Coplanar waveguide-fed uniplanar trapezoidal antenna with linear and circular polarization. *IEEE Transactions on Antennas and Propagation* **60**, 2522–2526.
7. **Zhang L, Jiao YC, Ding Y, Chen B and Weng Z** (2013) B.: CPW-Fed broadband circularly polarized planar monopole antenna with improved ground-plane structure. *IEEE Transactions on Antennas and Propagation* **61**, 4824–4828.
8. **Ding K, Guo YX and Gao C** (2017) CPW-Fed wideband circularly polarized printed monopole antenna with open loop and asymmetric ground plane. *IEEE Antennas and Wireless Propagation Letters* **16**, 833–836.
9. **Jan JY, Pan CY, Chiu KY and Chen HM** (2013) Broadband CPW-Fed circularly-polarized slot antenna with an open slot. *IEEE Transactions on Antennas and Propagation* **61**, 1418–1422.
10. **Ellis MS, Zhao Z, Wu J, Ding X, Nie Z and Liu QH** (2015) A novel simple and compact microstrip-fed circularly polarized wide slot antenna with wide axial ratio bandwidth for C-band applications. *IEEE Transactions on Antennas and Propagation* **64**, 1552–1555.
11. **Nosrati M and Tavassolian N** (2017) Miniaturized circularly polarized square slot antenna with enhanced axial-ratio bandwidth using an antipodal Y-strip. *IEEE Antennas and Wireless Propagation Letters* **16**, 817–820.
12. **Mushiake Y** (1992) Self-complementary antennas. *IEEE Antennas and Propagation Magazine* **34**, 23–29.
13. **Pu X, Fujimoto K and Shiming L** (2002) Performance of quasi-self-complementary antenna using a monopole and a slot. *Antennas and Propagation Society International Symposium* **2**, 464–467.
14. **Guo L, Wang S, Chen X-D and Parini C** (2009) A small printed quasi-self-complementary antenna for ultrawideband systems. *IEEE Antennas and Wireless Propagation Letters* **8**, 554–557.
15. **Guo L** (2008) Study of printed quasi-self-complementary antenna for ultra-wideband systems. *Electronics Letters* **44**, 511–512.
16. **Lin CC, Huang CY and Chen GH** (2013) Obtuse pie-shaped quasi-self-complementary antenna for WLAN applications. *IEEE Antennas and Wireless Propagation Letters* **12**, 353–355.
17. **Toh BY, Cahill R and Fusco VF** (2003) Understanding and measuring circular polarization. *IEEE Transactions on Education* **46**, 313–318.



Gunjan Srivastava received her Ph.D. degree from the Indian Institute of Technology (Indian School of Mines), Dhanbad, India in Microwave Engineering in 2016. At present, she is working as Women Scientist in the Department of E&ECE at the Indian Institute of Technology (IIT Kharagpur). She has authored or co-authored over 10 peer-reviewed international journal and conference papers. Her main research interests are design of ultra-wideband, reconfigurable, and MIMO antennas.

https://doi.org/10.1017/S175907871800106X Published online by Cambridge University Press